Chapter 1 Effect of leading edge spherical tubercles on the aerodynamic performance of a 2D wind turbine airfoil at low reynolds numbers using computational fluid dynamics

Capítulo 1 Análisis numérico de la influencia de las protuberancias esféricas en la eficiencia aerodinámica de un perfil 2D de turbina eólica a números de reynolds bajos

BENAVIDES-ZADOROZHNA, David Alexander†*, BENAVIDES, Olena, SIERRA GRAJEDA, Juan Manuel Tadeo, FIGUEROA-RAMÍREZ, Sandra Jazmín

Universidad Autónoma del Carmen

ID 1st Author: *David Alexander, Benavides-Zadorozhna* / **ORC ID**: 0000-0002-3240-1322, **CVU CONAHCYT ID**: 1231482

ID 1st Co-author: *Olena, Benavides* / **ORC ID**: 0000-0002-8124-0326, **CVU CONAHCYT ID**: 339830

ID 2nd Co-author: *Juan Manuel Tadeo, Sierra-Grajeda* / **ORC ID**: 0000-0002-0565-6450, **CVU CONAHCYT ID**: 219284

ID 3rd Co-author: *Sandra Jazmín, Figueroa-Ramírez* / **ORC ID**: 0000-0003-1368-1741, **CVU CONAHCYT ID**: 164797

DOI: 10.35429/H.2023.6.1.8

D. Benavides, O. Benavides, J. Sierra and S. Figueroa

*120134@mail.unacar.mx

S. Vargas, S. Figueroa, C. Patiño and J. Sierra (AA. VV.) Engineering and Applied Sciences. Handbooks-TI-©ECORFAN-Mexico, Mexico City, 2023

Abstract

The majority of wind power is currently produced on high wind speed sites by large wind turbine, whereas small wind turbines often operate in light wind conditions. Small capacity wind turbines have not received the same engineering attention as their large counterparts. This is partially due to a number of unique problems that small wind turbines experience. The most relevant are: low operating Reynolds number (Re<500,000) and high angles of attack. Several studies have suggested that flow control devices such as the spherical tubercle could be used to increase lift before stall and generate more power in such situations. The aim of this study is to determine the effect of tubercle amplitude on aerodynamic performance of an airfoil at low-Re numbers (Re=300,000 & Re=400,000). Three amplitudes were considered in this study: A_1=0.005c, A_2=0.01c, and A_3=0.03c. A detailed 2D simulation study is carried out using a calibrated Transition SST k-ω turbulence model to obtain aerodynamic coefficients and flow characteristics. Results indicate that small tubercles perform better overall than larger tubercles. The airfoil with the smallest tubercle outperforms the unmodified airfoil at both studied Reynolds numbers at angles of attack 0° – 4°. The analysis of the aerodynamic coefficients indicates that the improvement of the aerodynamic performance of the airfoils with tubercles is due to the reduction of the drag coefficient. Pressure, intermittency and wall shear stress contours suggest that the overall drag reduction is achieved through the decrease of friction drag.

Computational Fluid Dynamics, Spherical Tubercles, Airfoil Simulation

Resumen

En la actualidad, la mayor parte de la energía eólica se produce en emplazamientos con vientos fuertes mediante grandes aerogeneradores, mientras que los pequeños suelen funcionar con vientos flojos. Los aerogeneradores de pequeña potencia no han recibido la misma atención técnica que sus homólogos de gran tamaño. Esto se debe en parte a una serie de problemas específicos que experimentan los aerogeneradores pequeños. Los más importantes son el bajo número de Reynolds operativo (Re<500.000) y los elevados ángulos de ataque. Varios estudios han sugerido que los dispositivos de control de flujo, como el tubérculo esférico, podrían utilizarse para aumentar la sustentación antes de la entrada en pérdida y generar más potencia en estas situaciones. El objetivo de este estudio es determinar el efecto de la amplitud del tubérculo en el rendimiento aerodinámico de un perfil aerodinámico con números de Re bajos (Re=300.000 y Re=400.000). En este estudio se consideraron tres amplitudes: A1=0,005c, A2=0,01c, y A3=0,03c. Se lleva a cabo un estudio detallado de simulación 2D utilizando un modelo de turbulencia k-ω de Transition SST calibrado para obtener los coeficientes aerodinámicos y las características del flujo. Los resultados indican que los tubérculos pequeños presentan un mejor comportamiento general que los tubérculos más grandes. El perfil con el tubérculo más pequeño supera al perfil no modificado en los dos números de Reynolds estudiados para ángulos de ataque de 0° - 4°. El análisis de los coeficientes aerodinámicos indica que la mejora del rendimiento aerodinámico de los perfiles con tubérculos se debe a la reducción del coeficiente de resistencia. Los contornos de presión, intermitencia y esfuerzo cortante de pared sugieren que la reducción global de la resistencia aerodinámica se consigue mediante la disminución de la resistencia por fricción.

Dinámica de fluidos computacional, Tubérculos esféricos, Simulación de perfiles aerodinámicos

Introduction

Flow control devices arise from the need to manipulate a flow field to achieve a specific design goal. These devices are classified as passive if they require no additional power input and active if they require additional power to operate. Passive flow control devices modify the geometric shape of the wing to manipulate the pressure gradient. Tubercles are round protrusions on the leading edge that alter the flow field around a wing. These are classified as passive flow control devices. In addition to tubercles, other passive flow control devices such as leading edge extensions, pressure surface serrations, turbulent vortex generators, flaps and flexible coatings have also been studied. In contrast, active control involves the use of additional energy to operate devices such as actuators, which are often more complex and less economically effective, but offer performance advantages over passive control methods (Hansen *et al*., 2011).

It has been suggested that tubercles in humpback whale fins function as lift-enhancing devices. According to several researchers, the mechanism responsible for the improved aerodynamic performance is attributed to the formation of vortices along the flow, which increases momentum exchange in the boundary layer (Custodio, 2007; Johari *et al*., 2007; Miklosovik *et al*., 2004; Pedro and Kobayashi, 2008). This can lead to improvements in wing performance, such as maintaining flow stickiness for a wider range of angles of attack, stall point delay and a higher maximum lift coefficient with minimal drag penalties. Other mechanisms have been suggested, such as unequal separation properties (Fish and Lauder, 2006, Johari *et al*., 2007; Pedro and Kobayashi, 2008; van Nierop *et al*., 2008), altered pressure distribution over the wing surface (van Nierop *et al*., 2008) and vortex lift (Miklosovic and Murray, 2007). In addition, it has been suggested that the incorporation of tubercles could reduce noise.

Small wind turbines often operate in light wind conditions, where the turbine blade experiences a low Reynolds number (Re <500,000) and therefore the boundary layer over much of the suction side (top surface of the airfoil) is laminar and cannot overcome the strong adverse pressure gradient (Marty, 2014). Therefore, the boundary layer can separate and create a laminar separation bubble (LSB) where the transition from laminar to turbulent flow is triggered (Marty, 2014). Once the transition to turbulence is reached, the flow re-attaches to the surface, but in some scenarios, the separated flow may not be able to re-attach to the surface and this may lead to an early stall (Karasu *et al*., 2018). Therefore, tubercles could be used to increase lift before stall and generate more power in these situations. Measurements have already been conducted on wind turbines with tubers and have indicated that there is a potential for a substantial increase in electrical power production, leading to a higher annual energy production. The background studies to the present one have quite substantial experimental requirements. To obtain more accurate measurements of smaller scale and more sensitive flows, finer instrumentation needs to be added and the complexity of the flow needs to be increased, which can lead to additional experimental errors. Therefore, numerical experimental methods emerge as viable alternatives to experimentation. Numerical simulations are more accessible, practical, systematic and reliable.

The objective of this study is to evaluate the performance of leading edge profiles with spherical tubercles at low Reynolds numbers (Re = 300,000 and 400,000) using computational fluid dynamics. Improvements in lift-to-drag ratios were achieved for small and medium-sized tubercles at the Reynolds numbers studied. These findings support the fact that leading edge profiles with tubercles could have a practical application in small wind turbines.

Methodology and Modelling

This section discusses the creation of the geometry, the domain configuration, and the transition and turbulence model. An established and reliable airfoil within the wind energy industry is the DU93W210 airfoil (coordinates provided by (Tang, 2012)), which will have the nomenclature A0. The proposed amplitudes for the spherical tubercles are defined in terms of the chord length, and their nomenclatures are: A1 = 0.005c, A2 = 0.01c and A3 = 0.03c where the chord length is 0.6135 m.

1. Domain design

A rectangular domain is created around the airfoil with a width equal to the airfoil width. The inlet and outlet boundaries are kept at a distance of 10c (-x) and 12c (x) from the leading edge of the airfoil. The domain extends 10c above and below the profile to avoid confinement effects. A triangular mesh is generated around the airfoil with refinement zones around the airfoil and towards the flow out of the airfoil tail. The inflation layer around the airfoil was created with the first cell height method, where the desired y^+ value was set to 0.4 to capture the viscous underlayer. Additionally, the desired y^+ value is kept the same for all angles of attack because the calculated y^+ value does not exceed the $y^+ \sim 1$ criterion. The first cell height method uses the Reynolds number based on the characteristic scales of the geometry to calculate the wall friction coefficient C_f. It is therefore important to define the characteristic scales of the geometry, in this case it would be the chord length of the airfoil; L = 0,6135 m.

El The process for calculating and defining the value of y^+ is described in detail in the literature (Leading Engineering Application Providers, 2013). The height of the first layer is set to $1{,}8335 \times 10^{-5}$ m, and to keep the aspect ratio below 50, the airfoil is divided into 0.0009166 m elements. Thirty layers of inflation were created around the airfoil. The mesh quality achieved through this process is almost the same for all models.

The parameters to be evaluated are: average skewness, aspect ratio and orthogonal quality for each airfoil at an angle of attack of 0◦. According to the literature presented in Fluent (2009a), the mesh quality is excellent. The number of elements is the order $2.5 - 2.6 \times 10^6$, the number of nodes $1.27 - 1.35 \times 10^6$, lhe average obliquity quality is of the order of 8×10^{-2}, the aspect ratio quality is 1.42 and, finally, the orthogonal quality is 0.95.

2. Modelling of transition phenomena and turbulence

Developed by Menter *et al*. (2006) and Langtry *et al*. (2006b, c) the Transition SST k - ω turbulence model is used to model turbulent flows where a significant proportion of the boundary layer is laminar, this is very important for aerodynamic applications at moderate Reynolds numbers Re (∼ 105). In this Reynolds number regime, a significant proportion of the boundary layer is laminar and has an effect on the solution. Modelling the transition flows and the laminar flow region near the wall is of particular importance for the wind energy industry, because wind turbine blades depend on the aerodynamic performance of the airfoil surfaces. If the airfoil is optimised to operate at low Reynolds numbers, that could lead to an increase in electrical power output, leading to a higher annual energy production (Mauro *et al*., 2017). The Transition SST k - ω model was developed with these needs in mind. Previous work has shown excellent accuracy of the four-equation Transition SST k-ω turbulence model. The formulation is based on the well-known k - ω SST turbulence model with two additional transport equations. The first is the intermittency transport equation γ (equation (1)), which is used to trigger the transition process. The production term Pγ (eq. (2)) controls the length of the transition region, and the dissipation term Dγ dissipates the intermittency fluctuations, allowing the boundary layer to become laminar again.

$$\frac{\partial(\rho\gamma)}{\partial t} + \nabla \cdot (\rho U\gamma) = \nabla \cdot \left(\left(u + \frac{u_t}{\sigma_\gamma}\right)\nabla_\gamma\right) + P_\gamma - D_\gamma \tag{1}$$

$$P_{\gamma,1} = F_{length} c_{a1} \rho S (\gamma F_{onset})^{c_a} (1 - c_{e1}\gamma) \tag{2}$$

$$F_{onset1} = \frac{Re_v}{2.193 Re_{\theta c}} \tag{3}$$

The second is the transport equation for the transition momentum thickness Reynolds number (Eq. (5)), this equation defines a transition Reynolds number based on the momentum thickness. The formulation of the Transition SST k - ω model is presented extensively in Langtry *et al*. (2006b, c) and Langtry and Menter (2005), therefore, only a brief review of what is of particular interest for this work is discussed here.

$$\frac{\partial(\rho\overline{Re}_{\theta,t})}{\partial t} + \nabla \cdot \left(\rho U \overline{Re}_{\theta,t}\right) = \nabla \cdot \left[\left(\mu + \frac{\mu_t}{\sigma_{\theta,t}}\right)\nabla\overline{Re}_{\theta,t}\right] + P_{\theta t} \tag{4}$$

$$P_{\theta t} = 0.03 \frac{\rho}{t}\left(Re_{\theta,t} - \overline{Re}_{\theta,t}\right)\left(1 - F_{\theta,t}\right) \tag{5}$$

Since the proposed transport equations do not model the physics of the transition, the source term is included to enforce $\overline{Re}_{\theta t}$ to take the empirical value of $Re_{\theta t}$, (everywhere in the flow except the boundary layer, because there the source is turned off). $F_{\theta t}$ is the same as the mixing function in the turbulence model SST k – ω. Where $F_{\theta,t} = 0$ in the free stream and $F_{\theta,t} = 1$ near the wall. The Reynolds number based on the thrust thickness is a measure of the distance from the leading edge of the airfoil to a certain point on the airfoil surface. Also, since the Reynolds number is a measure of distances, there will be a Reynolds number at which the transition occurs and this is denoted by $Re_{\theta t}$.

At a certain Reynolds number based on the thickness of the impulse from the leading edge, fluctuations will start to occur, this quantity is given by $Re_{\theta c}$. The suffix c is for the Reynolds number at which turbulent fluctuations start (critical Reynolds number), and this is before the transition occurs. The use of reliable empirical relationships (source terms) is needed to accurately calculate the local values of $Re_{\theta c}$ y $Re_{\theta t}$. The fact that the turbulence model is based on empirical relationships makes it suitable for the simulation of aerodynamic surfaces at low Reynolds numbers, if appropriate values are provided (Langtry and Menter, 2005).

Furthermore, scientific literature showed that, the use of transition turbulence models, at low Reynolds numbers (Aftab and Ahmad, 2017; Benini and Ponza, 2010), is essential to obtain an adequate CFD model of the airfoil and rotor airfoil aerodynamic behaviours. Moreover, a CFD study by Mauro *et al*. (2017) demonstrates an exceptional agreement between experimental data and simulation results of the calibrated Transition SST k - ω turbulence model. The calibration of the local correlation parameters $Re_{\theta c}$ y F_{length} was achieved through a micro-genetic algorithm. Correct calibration of these parameters allows accurate prediction of stagnation and flow separation, as well as obtaining reliable lift and drag coefficients that can be used in 2D CFD models. The authors claim that the calibrated local correlations can be used for the simulation of other aerodynamic surfaces within the Reynolds number range 300,000 and 1 million. This, therefore, will give this work experimental support. $Re_{\theta c}$ y F_{length} for a given Reynolds number can be defined as (Mauro *et al*., 2017):

$$Re_{\theta c} = 3.9592e^{-16}Re^3 - 9.598e^{-9}Re^2 + 6.884e^{-4}Re + 984.0408 \quad (6)$$

$$F_{length} = 1.7808e^{-15}Re^3 - 2.1514e^{-9}Re^2 + 8.132e^{-4}Re - 91.2135 \quad (7)$$

3. CFD solver setup

Commercial simulation software was used to perform a steady state analysis for angles of attack of 0◦-15◦ (in steps of 2◦), considering the Transition SST k - ω model. The Transition SST k - ω model has been well tested and designed for low Reynolds number aerodynamic applications. The Transition SST k - ω model was chosen over the other turbulence models because of its ability to accurately predict boundary layer velocity and boundary layer separation. Low Reynolds number models are also necessary for accurate pressure drop or drag calculations. The Reynolds numbers studied in this work are 300,000 and 400,000. Therefore, the inlet velocity is set at 7 m/s and 9.5 m/s respectively. For all simulations, the solver was set up as a steady-state, pressure-based, ACOPLED algorithm scheme with an absolute velocity formulation. The fluid is defined as air with density equal to 1.225 kg/m^3 and, dynamic viscosity $\mu = 1.7894 \times 10^{-5} \frac{N \cdot s}{m^2}$. The turbulence intensity (TI = 0.1%) and turbulent viscosity ratio (TVR = 10) were defined across the velocity boundary.

This lower TI corresponds to that of a typical low-turbulence wind tunnel and implies a natural or separation-induced transition mechanism, according to Langtry and Menter (2005) and Langtry *et al*. (2006a). A least-squares cell-based scheme was used for the spatial discretisation of the gradient, while second-order upwind schemes were used for the pressure, momentum and turbulence equations. In the steady-state coupling solver, the Courant number allows control of the sub-iteration time step. In other words, even if the steady-state solver is used, a transient sub-iteration is performed and the time scale of the simulation can be adapted to the flow time scale. In attached flow conditions, the Courant number was set to 25. At AoAs > 10◦ the instability generated by stall and vortices was noted. Under these conditions, the Courant number must be reduced to adapt the time scale so that an accurate average of the lift and drag coefficients can be obtained. A convergence criterion of O(-4) on all residuals of the dependent variables is accepted as adequate for the present airfoil simulation. To provide the local correlation parameters F_{length} y $Re_{\theta c}$, a user-defined function (UFD) in C language was written and interpreted.

Results and discussion

The behaviour of spherical tuber leading edge profiles is consistent with previous results (Aftab and Ahmad, 2017; Johari *et al*., 2007). As anticipated, small tubercles perform more efficiently in general than tubercles with larger amplitudes. The A1 airfoil showed a minor improvement in lift-to-drag ratio from AoA 0◦-4◦ at a Reynolds number of 300,000 (Graph 1a). However, past AoA 4◦, the improvements become less noticeable and at AoA 6◦, the aerodynamic performance starts to deteriorate. Airfoil A3 showed the greatest improvement at an angle of attack of 0◦, with a 12.86 % increase in lift-to-drag ratio; beyond this angle of attack, the airfoil suffers a significant deterioration in aerodynamic performance. The A2 airfoil shows no significant improvement in lift-to-drag ratio and instead experiences an overall decrease in aerodynamic performance for all angles of attack. Note that the tubercles anticipate the peak of the lift-to-drag ratio and do not retard the stall angle in this case. The maximum lift-to-drag ratio point for the unmodified airfoil is at AoA 8◦, while for A1 the maximum lift-to-drag ratio is at AoA 6◦, and for A2 and A3 at AoA 4◦.

This is in good agreement with Johari *et al*. (2007) and Miklosovik *et al*. (2004) TLE airfoils have lower stall angles and lower maximum lift coefficients than their unmodified versions. The A1 airfoil data follow a pattern and suggest that the non-intrusive tubercles have a small reduction in lift coefficient, but a significant decrease in drag. Similar conclusions can be drawn when analysing the lift-drag ratio when Re = 400,000 (Graph 1b).

Analysis of the static pressure and intermittency contours revealed that the type of drag that has the most significant impact in this case is pressure drag. Observe Fig. 2 (a1) and (a2), as the fluid passes over the surface of the airfoil sphere A3, it initially accelerates and therefore the pressure decreases in the direction of flow. Beyond a certain point, the flow begins to decelerate and therefore the pressure in the direction of flow increases; this pressure increase is called the adverse pressure gradient and has a significant effect on the flow near the wall. The turbulence produced by the tubercle promotes momentum exchange between the boundary layers and that is why the A3 airfoil achieves a 3.31% increase in the lift coefficient at AoA 0°. As the angle of attack increases, the pressure and drag induced become more noticeable in Fig. 2 (b1) and (b2). If the pressure increase is large enough, the flow will reverse direction and, since it cannot travel backwards, due to the approaching fluid, it detaches from the surface, resulting in flow separation (Houghton *et al*., 2017). This explains why the A3 airfoil experiences such a dramatic increase in drag beyond AoA 0°. Note in Fig. 2 (a2) that the laminar flow layer remains attached to the upper surface of the airfoil, while at an angle of attack of 8° Fig. 2 (b2), the vortices produce so much turbulence that they manage to break through the laminar flow layer, resulting in flow separation.

Graph 1 Lift-drag coefficient a) Re=300,000 and b) Re=400,000

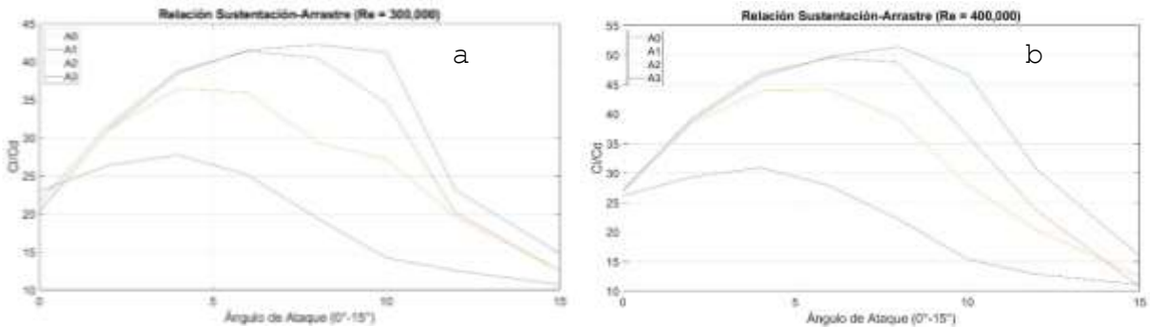

The tubercle in the A1 airfoil distributes the pressure forces in such a way that it thickens the laminar boundary layer of AoA 0° - 8°. However, this becomes less noticeable as the angle of attack increases. Due to the turbulence produced by the tubercle, the laminar flow layer is broken and the flow becomes unstable.

Graph 2 Pressure and intermittency contours for profile A3 a) AoA 0° and b) AoA 8°.

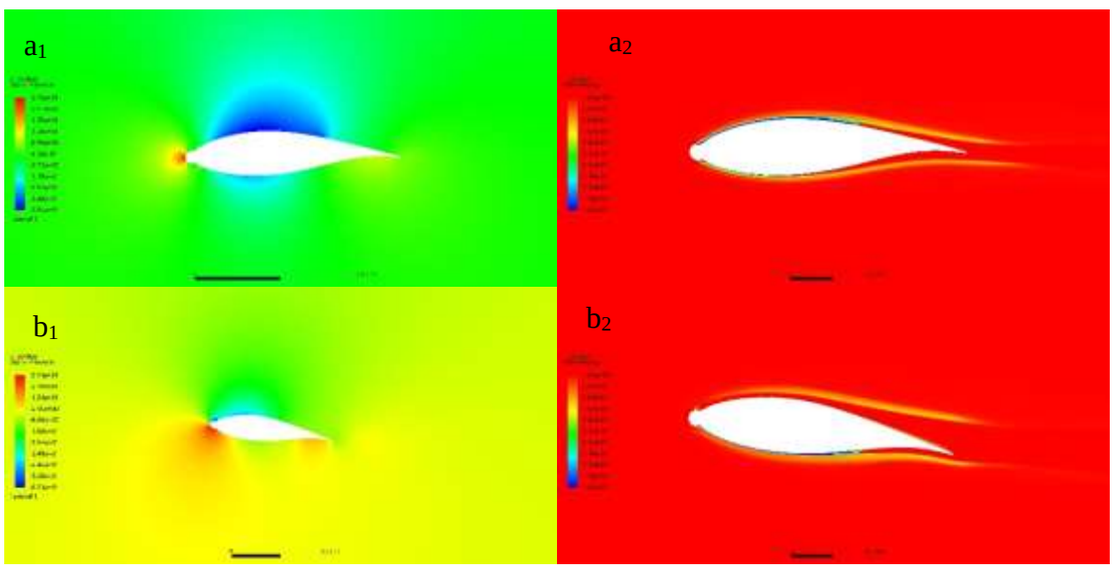

Conclusions

This paper investigated the aerodynamic performance of airfoils with spherical tubercles at the leading edges by numerical analysis of three different amplitudes and comparison with the unmodified airfoil. The Reynolds numbers studied in this work are $Re = 3 \times 10^5$ and $Re = 4 \times 10^5$. The Transition SST k - ω turbulence model was used to model the turbulence due to its ability to accurately predict the flow separation in the low Reynolds number regime, and the local correlation parameters F_{length} and $Re_{\theta c}$, were defined with the polynomial functions given by the work of Mauro *et al*. (2017). Smaller amplitude tubercles perform better overall than larger ones, but their overall efficiency does not exceed the unmodified aerodynamic surface area. The improved lift-to-drag ratio is attributed to reduced surface frictional drag. Static pressure contours, wall shear stress and intermittency contours suggest that the reduction in surface friction drag is caused by a more favourable pressure distribution around the airfoil. The correct pressure distribution allows for a thicker laminar boundary layer, which in turn helps to reduce wall frictional drag. Our work clearly has some limitations, as only a part of the full tubercle effect was studied in this paper. Despite this, our work could be the basis for developing methods to optimise tuber shape and size by providing accurate databases of aerodynamic coefficients of 2D aerodynamic surfaces with spherical tuber leading edges.

Acknowledgements

The work described in this article was funded by the Universidad Autónoma del Carmen. We are grateful to CONACyT for providing the computational resources used to carry out this work through Project No. 254667 "Consolidation of the Southeast Renewable Energy Laboratory" LENERSE."

References

Aftab, S., Ahmad, K.A., 2017. CFD study on NACA 4415 airfoil implementing spherical and sinusoidal Tubercle Leading Edge. PLoS One 12 (8), e0183456. http://dx.doi.org/10.1371/journal.pone.0183456

Benini, E., Ponza, R., Laminar to turbulent boundary layer transition investigation on a supercritical airfoil using the γ -θ Transitional Model 40th Fluid Dynamics Conference and Exhibit, 28 June-1 2010, Chicago, Illinois, AIAA 2010-4289.

Custodio, D., 2007. The Effect of Humpback Whale-Like Leading Edge Protuberances on Hydrofoil Performance (M.S. Thesis). Worcester Polytechnic Inst., Worcester, MA.

Fish, F.E., Battle, J.M., 1995. Hydrodynamic design of the humpback whale flipper. J. Morphol. 225, 51–60. http://dx.doi.org/10.1002/jmor.1052250105.

Fish, F.E., Lauder, G.V., 2006. Passive and interactive flow control by swimming fishes and mammals. Annu. Rev. Fluid Mech. 38, 193–224.

Fluent, 2009a. ANSYS FLUENT 12.0 Theory Guide. ANSYS Inc., Section 6.2.2 Mesh Quality.

Hansen, K.L., Kelso, R.M., Dally, B.B., 2011. Performance variations of leadingedge tubercles for distinct airfoil profiles. AIAA J. 49 (1), 185–194. http://dx.doi.org/10.2514/1.j050631.

Houghton, E.L., Carpenter, P.W., Collicott, Steven H., Valentine, Daniel T., 2017. Chapter 1 - Basic concepts and definitions. In: Houghton, E.L., Carpenter, P.W., Collicott, Steven H., Valentine, Daniel T. (Eds.), Aerodynamics for Engineering Students, seventh ed. Butterworth-Heinemann, ISBN:9780081001943, pp. 1–86. http://dx.doi.org/10.1016/B978-0-08-100194-3.00001-8.

Johari, Hamid, Henoch, Charles, Custodio, Derrick, Levshin, Alexandra, 2007. Effects of leading-edge protuberances on airfoil performance. AIAA J. 45, 2634–2642. http://dx.doi.org/10.2514/1.28497.

Karasu, İ., Özden, M., Genç, M.S., 2018. Performance assessment of transition models for three-dimensional flow over NACA4412 wings at low Reynolds numbers. ASME J. Fluids Eng. 140 (12), 121102. http://dx.doi.org/10.1115/1.4040228.

Langtry, Robin, Gola, Janusz, Menter, Florian, 2006a. Predicting 2D airfoil and 3D wind turbine rotor performance using a transition model for general CFD codes. In: 44th AIAA Aerospace Sciences Meeting and Exhibit. AIAA 2006-395.

Langtry, Robin, Menter, Florian, 2005. Transition modeling for general CFD applications in aeronautics. In: AIAA 2005-522 43rd AIAA Aerospace Sciences Meeting and Exhibit.

Langtry, R.B., Menter, F.R., Likki, S.R., Suzen, Y.B., Huang, P.G., Volker, S., 2006b. A correlation-based transition model using local variables – Part I: model formulation In: Vienna, ASME Paper No. ASME-GT2004-53452.

Langtry, R.B., Menter, F.R., Likki, S.R., Suzen, Y.B., Huang, P.G., Volker, S., 2006c. A correlation-based transition model using local variables – Part II: test cases and industrial applications. ASME J. Turbomach. 128 (3), 423–434.

Leading Engineering Application Providers, 2013. Tips & Tricks: Estimating the first cell height for correct Y+. Available at: https://www.computationalfluiddynamics.com.au/tips-tricks-cfd-estimate-first-cellheight/.

Marty, J., 2014. Numerical investigations of separation-induced transition on high-lift low-pressure turbine using RANS and LES methods. Proc. Inst. Mech. Eng. A 39, ff. http://dx.doi.org/10.1177/0957650914548741ff, ffhal01080267f.

Mauro, S., Lanzafame, R., Messina, M., et al., 2017. Transition turbulence model calibration for wind turbine airfoil characterization through the use of a Micro-Genetic Algorithm. Int. J. Energy Environ. Eng. 8, 359–374. http://dx.doi.org/10.1007/s40095-017-0248-2.

Miklosovic, D.S., Murray, M.M., 2007. Experimental evaluation of sinusoidal leading edges. J. Aircr. 44, 1404–1407.

Miklosovik, D.S., Murray, M.M., Howle, L.E., Fish, F.E., 2004. Leading edge tubercles delay stall on humback whale flippers. Phys. Fluids 16 (5), L39–L42. http://dx.doi.org/10.1063/1.1688341.

Pedro, H.T.C., Kobayashi, M.H., 2008. Numerical study of stall delay on Humpback whale flippers. In: Proceedings of 46th AIAA Aerospace Sciences Meeting and Exhibit, 7-10th January, Reno, Nevada.

Tang, Xinzi, 2012. Aerodynamic Design and Analysis of Small Horizontal Wind Turbine Blades (Ph.D. thesis). University of Central Lancashire, UK, Available at: http://clok.uclan.ac.uk/7127/1/Tang%20Xinzi%20Final%20eThesis%20%28Master%20Copy%29.pdf.

van Nierop, Ernst, Alben, Silas, Brenner, Michael, 2008. How bumps on whale flippers delay stall: An aerodynamic model. Phys. Rev. Lett. 100, 054502